


Dissecting interplays between *Vitis vinifera* L. and grapevine virus B (GVB) under field conditions

WALTER CHITARRA ^{1,2,*}, DANILA CUOZZO^{2,3}, ALESSANDRA FERRANDINO³, FRANCESCA SECCHI³, SABRINA PALMANO², IRENE PERRONE², PAOLO BOCCACCI², CHIARA PAGLIARANI², IVANA GRIBAUDO², FRANCO MANNINI² AND GIORGIO GAMBINO²

¹Research Centre for Viticulture and Enology, Council for Agricultural Research and Economics (CREA-VE), Via XVIII Aprile 26, Conegliano, 31015, Italy

²Institute for Sustainable Plant Protection, National Research Council (IPSP-CNR), Strada delle Cacce 73, Torino, 10135, Italy

³Department of Agricultural, Forest, and Food Sciences, University of Turin (DISAFA), Largo Paolo Braccini 2, Grugliasco, 10095, Italy

SUMMARY

Plant virus infections are often difficult to characterize as they result from a complex molecular and physiological interplay between a pathogen and its host. In this study, the impact of the phloem-limited grapevine virus B (GVB) on the *Vitis vinifera* L. wine-red cultivar Albarossa was analysed under field conditions. Trials were carried out over two growing seasons by combining agronomic, molecular, biochemical and ecophysiological approaches. The data showed that GVB did not induce macroscopic symptoms on 'Albarossa', but affected the ecophysiological performances of vines in terms of assimilation rates, particularly at the end of the season, without compromising yield and vigour. In GVB-infected plants, the accumulation of soluble carbohydrates in the leaves and transcriptional changes in sugar- and photosynthetic-related genes seemed to trigger defence responses similar to those observed in plants infected by phytoplasmas, although to a lesser extent. In addition, GVB activated berry secondary metabolism. In particular, total anthocyanins and their acetylated forms accumulated at higher levels in GVB-infected than in GVB-free berries, consistent with the expression profiles of the related biosynthetic genes. These results contribute to improve our understanding of the multifaceted grapevine–virus interaction.

Keywords: anthocyanins, gas exchange, grapevine, plant–virus interaction, sugar signalling.

INTRODUCTION

Plant viruses are obligate biotrophic agents often capable of causing extensive damage and serious economic losses to many cultivated crops (Moon and Park, 2016). A number of studies have reported virus infections mainly as pathogenic relationships

without any beneficial effects for plant hosts, which offer their cellular apparatus to support virus movement and proliferation (Wang, 2015; Zhao *et al.*, 2016). The massive titre of virions facilitates their survival and transmission, although plants can react to the infection by implementing several strategies to hinder and/or eradicate these pathogens (Armijo *et al.*, 2016; Hipper *et al.*, 2013; Moon and Park, 2016; Pumplin and Voinnet, 2013). Moreover, some pathogenic viruses have developed molecular systems able to bypass the plant defence machinery, thus leading to successful systemic infections, even up to host death (Miozzi *et al.*, 2013). Immune responses against viral pathogens rely on the recognition of pathogen-associated molecular patterns (PAMPs) by pattern recognition receptors (PRRs), inducing PAMP-triggered immunity (PTI) (as reviewed by Moon and Park, 2016). Moreover, in detail, most of the above cited processes involve RNA silencing as a conserved mechanism, in which small non-coding RNAs (sRNAs) directly regulate gene expression and finely tune biochemical and physiological pathways crucial for the plant to react and/or adapt to biotic (Pantaleo *et al.*, 2016; Ruiz-Ferrer and Voinnet, 2009) or abiotic (Pagliarani *et al.*, 2017) factors. These natural plant defence strategies against virus invasion also imply the production of virus-derived small interfering RNAs (vsiRNAs) that guide Argonaute (AGO) complexes to inactivate viral genomes (Huang *et al.*, 2016). As a response, to counter plant defences, viruses encode viral suppressors of the RNA silencing machinery (VSRs), which promote their accumulation and movement within infected tissues (Csorba *et al.*, 2009; Hipper *et al.*, 2013).

To date, several studies have analysed the effects of pathogenic viruses in plants, including grapevine, by means of ecophysiological, molecular and biochemical approaches (e.g. El Aou-ouad *et al.*, 2016; Endeshaw *et al.*, 2014; Gambino *et al.*, 2012; Montero *et al.*, 2016a, b). In addition, during the last decade, researchers have started to consider the plants as holobionts, composed of complex micro- and microbiomes interacting with the environment as a unique organism and able to modulate

*Correspondence: Email: walter.chitarra@crea.gov.it

plant responses to biotic or abiotic factors (Dessaux *et al.*, 2016; Dicke, 2016). Accordingly, recent studies have highlighted the complexity of virus–host interaction, attesting that it goes beyond the classical binary host–pathogen relationship.

More recently, thanks to the advances in deep sequencing technologies and the discovery of new viruses, beneficial interactions between viruses and plants have also been reported (see review by Roossinck, 2011 and references therein). Indeed, in some cases, the plant–virus relationship can shift from antagonistic to mutualistic or beneficial in response to environmental changes. Curiously, over the years, this relationship can evolve and lead to symbiosis, in which the two entities merge, creating a new species with endogenized virus-like sequences in the host's genome, as observed in banana and wasps (Roossinck, 2015). In plants, viruses can increase the tolerance to bacterial pathogens (Shapiro *et al.*, 2013) or abiotic stresses, such as drought (Pantaleo *et al.*, 2016; Xu *et al.*, 2008), high soil temperatures (Márquez *et al.*, 2007) or cold stress (Xu *et al.*, 2008). In addition, plants are often infected by one or more asymptomatic virus(es), vertically transmitted, probably over very long periods of time, whose potential beneficial (or mutualistic) interaction with the host and its biology still need to be elucidated (Nerva *et al.*, 2017; Pradeu, 2016; Roossinck, 2012).

Grapevine (*Vitis* spp.) is a model plant to study plant–virus interactions in woody species in both controlled and field conditions (Perrone *et al.*, 2017). Grapevine represents one of the most economically important fruit crops in the world with very ancient origins and potentially infected by many viral entities (Mannini and Digiario, 2017; Martelli, 2017). As mentioned previously, several studies have been conducted on pathogenic viruses invading grapevines; nevertheless, in some environmental conditions and in specific grapevine genotype–virus strain combinations, some of these are harmless to the plant. For instance, transcriptomic and ecophysiological analyses on field-grown *Vitis vinifera* L. plants infected with grapevine rupestris stem pitting-associated virus (GRSPaV) revealed an interesting overlap with plant responses related to water and salinity stresses (Gambino *et al.*, 2012). In addition, in glasshouse conditions, GRSPaV-infected plants showed an increased tolerance to water stress, resulting in particular physiological traits and in the activation of peculiar microRNAs (miRNAs) (Pantaleo *et al.*, 2016). In addition, Repetto *et al.* (2012) demonstrated that grapevines infected with grapevine leafroll-associated virus-3 (GLRaV-3) display an increased resistance to the fungal pathogen *Plasmopara viticola*. Indeed, GLRaV-3 causes several detrimental effects in grapevine determined by a number of molecular and physiological changes (Gutha *et al.*, 2010; Montero *et al.*, 2016a; Vega *et al.*, 2011) which may hinder fungal pathogenicity. Altogether, these studies highlight the importance to deepen the biology underlying plant–virus interactions.

Of the close to 80 viral species identified in grapevine (Martelli, 2018), grapevine virus B (GVB), a member of the genus *Vitivirus*,

family *Betaflexiviridae*, is closely associated with corky bark disorder, one of the syndromes of rugose wood complex (Martelli, 2017). This phloem-limited virus can cause corky-like symptoms (i.e. swollen and longitudinally split cane wood and leaf reddening) on the LN33 grape hybrid (Courderc1613 × Thompson Seedless), and is transmitted by grafting or pseudococcid mealybugs (*Pseudococcus* ssp. and *Planococcus* ssp.) (Goszczyński, 2010). Although not particularly widespread, GVB is generally considered to be harmful as it potentially affects graft unions; this is the reason why the Italian regulations (DM 06/24/2008) list GVB amongst the viruses from which a selected grapevine clone must be free to be registered in the National Catalogue. The specific phenotypes of different genotypes infected by GVB (corky-like symptoms substantially limited to hybrid LN33 and the general asymptomatic behaviour of many *V. vinifera*–GVB combinations) can be related to specific, still unknown, molecular and physiological mechanisms. In this context, this study aimed to investigate and characterize the interplay between GVB and *V. vinifera* plants by comparing virus-infected vs. virus-free vines. In particular, we selected the wine-red cultivar 'Albarossa' grown under vineyard conditions and focused on the host responses triggered by the virus through a combination of agronomic, molecular, ecophysiological and biochemical approaches.

RESULTS

Quantification of GVB titre, climatic conditions and field parameters

At the beginning, the presence or absence of GVB was verified by reverse transcription-polymerase chain reaction (RT-PCR) in infected and healthy 'Albarossa' vines grafted onto the rootstock Kober 5BB. Similarly, the absence of other viruses [arabis mosaic virus (ArMV), grapevine fanleaf virus (GFLV), grapevine fleck virus (GFkV), grapevine virus A (GVA), grapevine leafroll-associated virus-1, -2, -3 (GLRaV-1, -2, -3)] was ascertained by RT-PCR in all tested vines. From the phenotypic point of view, both infected and GVB-free plants did not exhibit macroscopic alterations (Fig. S2, see Supporting Information), and corky-like symptoms were not detected at graft unions, as expected. The sequencing of GVB end-point RT-PCR products (Gambino and Gribaudo, 2006), corresponding to a partial sequence of ORF5, a putative RNA-binding protein, confirmed a high degree of heterogeneity of GVB (Fonseca *et al.*, 2016; Goszczyński, 2010). The GVB isolate infecting 'Albarossa' (AB.1, NCBI accession number MG725619) had 92.8% nucleotide sequence identity with isolate 94/971 (Fig. S3, see Supporting Information) from a corky bark-diseased vine in South Africa (Moskovitz *et al.*, 2008).

Moreover, during the whole 2016 season, the GVB titre was monitored by quantitative RT-PCR in leaf and berry samples and calculated as the relative expression ratio to the virus titre in leaf samples on 30th June 2016 (Fig. 1). GVB concentration in

leaves was similar in June and July, and progressively decreased in August and September. Conversely, in berry tissues, the viral RNA content was always higher than that measured in leaves, and its concentration increased significantly over the season, showing values almost 1000 times higher than those measured in June (Fig. 1).

Seasonal patterns of daily maximum temperature, maximum daily vapour pressure deficit (mVPD) and rainfall were also monitored in the experimental vineyard during both 2015 and 2016 (Fig. S1, see Supporting Information). The data obtained indicated that the 2 years were characterized by similar weather conditions, slightly cooler and wetter in 2015 than in 2016, particularly from July to September (Fig. S1). Agronomic parameters measured in 2015–2016 did not differ significantly between GVB-infected and healthy vines (Table 1). Yield, bunch weight and vegetative vigour were similar for the two groups of vines, but varied with year and environmental factors.

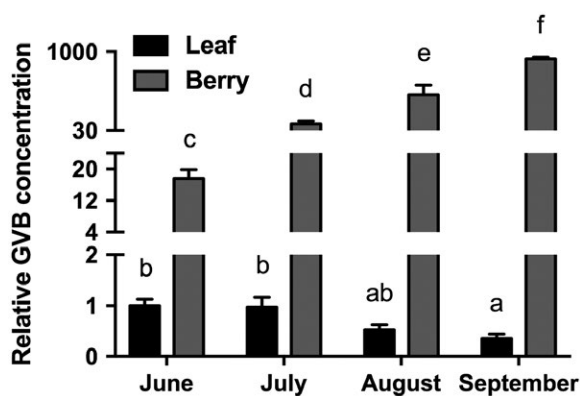


Fig. 1 Quantification of grapevine virus B (GVB) RNA in leaf (black columns) and berry (grey columns) of 'Albarossa' as determined by quantitative reverse transcription-polymerase chain reaction (RT-PCR). Samples were collected over the 2016 season and quantitative RT-PCR signals were normalized to *VvAct* and *VvUBI* transcripts. Data are presented as the mean \pm standard deviation (SD) ($n = 3$). Lowercase letters denote significant differences attested by Tukey's honestly significant difference (HSD) test ($P < 0.05$).

These results indicate that, over two seasons with similar climatic conditions, GVB-infected plants showed phenotypes (agronomic features) not significantly different from those of GVB-free vines. This lack of differences applied especially at the level of bunches and yield, although a time course realized in 2016 showed that virus accumulated at very high concentrations in berries.

Ecophysiological parameters, ribulose-1,5-bisphosphate carboxylase/oxygenase (Rubisco) content and expression of target genes involved in photosynthesis

During both years, the stem water potential (Ψ_{stem}) was measured on the studied vines and, irrespective of the sanitary status, values were stable over the time course of the experiment (around -0.5 MPa), thus attesting to the well-watered condition of the plants, which was not affected by virus presence and/or environment (Fig. S4, see Supporting Information). Unlike Ψ_{stem} , net photosynthesis (Pn) followed a decreasing trend from June to September (Fig. 2a). In particular, the infected grapevines had significantly lower Pn rates than GVB-free plants in August and September (Fig. 2a). Substomatal CO_2 concentrations (c_i) were, instead, similar for both groups of vines, with the exception of September, when significantly higher values were recorded for infected plants (Fig. 2b). In contrast, stomatal conductance (g_s) was always lower in GVB-infected plants, particularly in July (Fig. 2c).

To further explore the photosynthetic performances of selected plants, the Rubisco content was quantified on leaf samples and expressed in terms of density units. The results showed that the enzyme concentration was always higher in GVB-infected plants, although significant differences were observed only in September (Figs 2d and S5, see Supporting Information). In addition, the expression of two genes encoding a Rubisco activase (VIT_13s0019g02050) and a Chlorophyllase (VIT_07s0151g00110) was analysed by quantitative RT-PCR in leaf samples (Fig. 2e,f). The data indicated that, on GVB infection, the transcript accumulation of the *VvRubisco activase* gene

Table 1 Agronomic features of *Vitis vinifera* cv. 'Albarossa' monitored in the 2015 and 2016 growing seasons.

	Bunch weight (g)	Yield/plant (kg)	Pruned wood/plant (kg)
2015			
GVB-free	190.00 \pm 11.15 ^a	2.06 \pm 0.23 ^a	0.48 \pm 0.10 ^a
GVB-infected	184.00 \pm 6.47 ^a	2.16 \pm 0.13 ^a	0.61 \pm 0.05 ^a
2016			
GVB-free	283.00 \pm 6.29 ^a	3.91 \pm 0.41 ^a	0.56 \pm 0.06 ^a
GVB-infected	255.00 \pm 23.98 ^a	3.37 \pm 0.63 ^a	0.61 \pm 0.14 ^a

Letters reported for each value within the same column and for the same year indicate significant differences attested by Student's *t*-test ($P < 0.05$). Data are expressed as mean \pm standard deviation (SD) ($n = 6$).

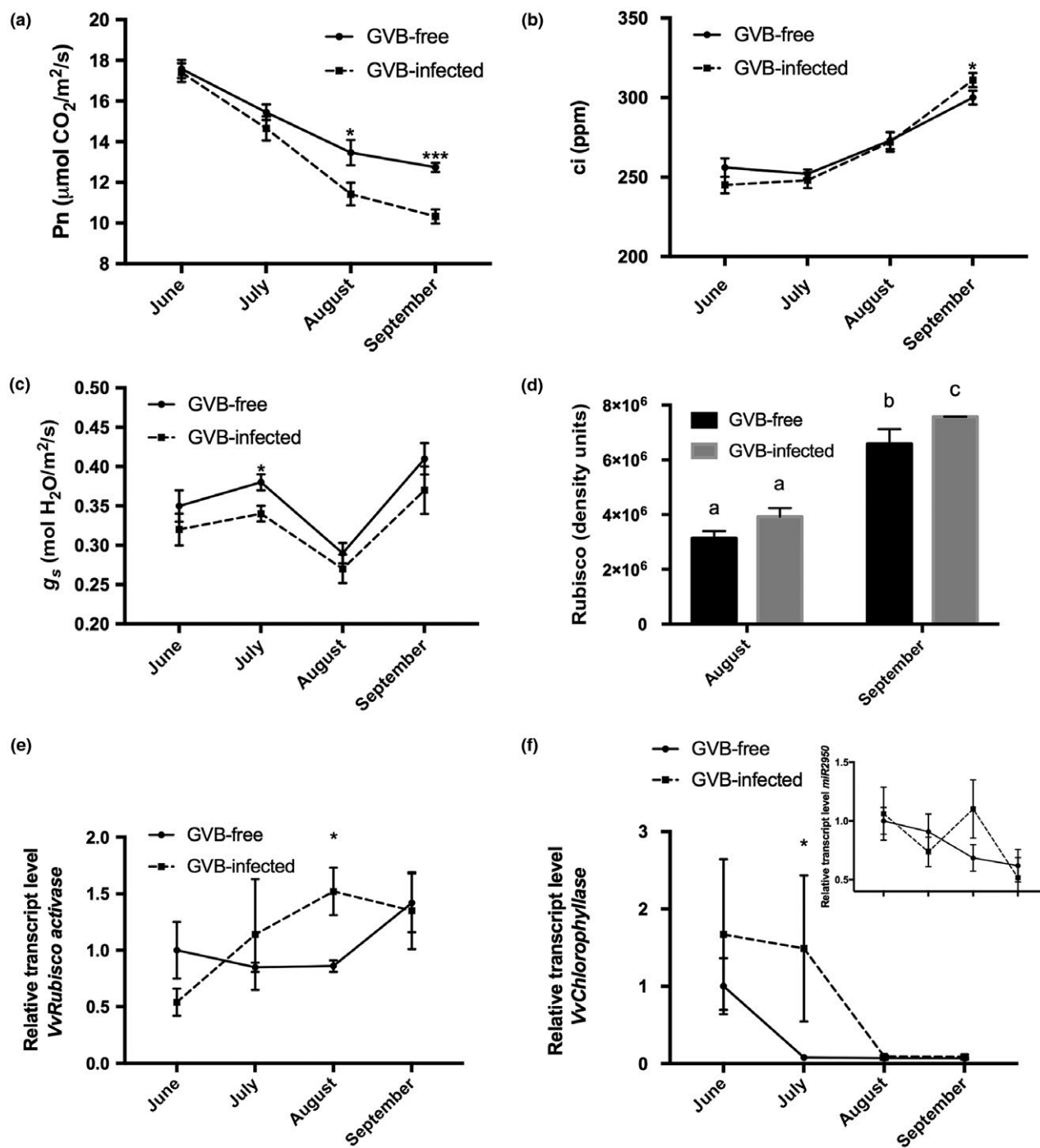


Fig. 2 Seasonal time course (2016) of carbon assimilation (net photosynthesis, Pn) (a), substomatal internal carbon concentration (substomatal CO_2 concentration, ci) (b) and stomatal conductance (g_s) (c) in grapevine virus B (GVB)-free (full line, filled circles) and GVB-infected (broken line, filled squares) 'Albarossa' plants. Data are expressed as the mean \pm standard deviation (SD) ($n = 6$). (d) Ribulose-1,5-bisphosphate carboxylase/oxygenase (Rubisco) quantification (density units) in samples collected at the end of August and September from GVB-free (black columns) and GVB-infected (grey columns) plants. Data are expressed as mean \pm SD ($n = 3$). Seasonal changes in the transcriptional profiles of (e) *VvRubisco activase* (VIT_13s0019g02050), (f) *miR2950* (inset) and its target transcript *VvChlorophyllase* (VIT_07s0151g00110) measured by quantitative reverse transcription-polymerase chain reaction (RT-PCR) in GVB-free (full line, filled circles) and GVB-infected (broken line, filled squares) leaves. Data are expressed as mean \pm SD ($n = 3$). Asterisks and lowercase letters denote significant differences between GVB-free and GVB-infected plants attested by two-tailed Student's *t*-test and Tukey's honestly significant difference (HSD) test ($P < 0.05$ or $P < 0.01$), respectively.

increased up to August, and then was almost stable until the end of September. Conversely, GVB-free samples showed lower expression levels of this gene over time, with the exception of the leaves taken at the end of September, where a strong activation of the gene was found, with values similar to those observed in infected plants (Fig. 2e). It is worth noting that GVB also induced the expression of *VvChlorophyllase* transcripts, which, during the first part of the season were highly up-regulated in infected vs. GVB-free plants (although significant differences were detectable only in July). In addition, although, in GVB-infected samples, the transcript accumulation of this gene collapsed after July, in the leaves of GVB-free vines, *VvChlorophyllase* transcript accumulation started to decrease at an earlier stage (Fig. 2f). Finally, knowing that *VvChlorophyllase* gene expression is post-transcriptionally regulated by the grapevine-specific miRNA miR2950 (Pantaleo *et al.*, 2016), the expression profile of this miRNA was studied. The results documented the existence of an

inverse relationship between miR2950 and its target gene, but exclusively in GVB-infected plants (Fig. 2f, inset).

Thus, GVB affects g_s and Pn rates mainly at the end of the season. Accordingly, at the molecular level, in GVB-infected plants, *VvRubisco activase* expression decreased late in the season, whereas *VvChlorophyllase* transcript accumulation followed a decreasing trend over the whole season, probably because of post-transcriptional regulation by miR2950.

Soluble carbohydrate content and expression of leaf target genes related to sugar metabolism, cell growth and development

Concentrations of soluble carbohydrates were quantified in samples collected in August and September 2016, when differences in gas exchange measurements between the two sets of plants were observed (Fig. 2a). The content of soluble carbohydrates measured in xylem sap samples increased significantly in

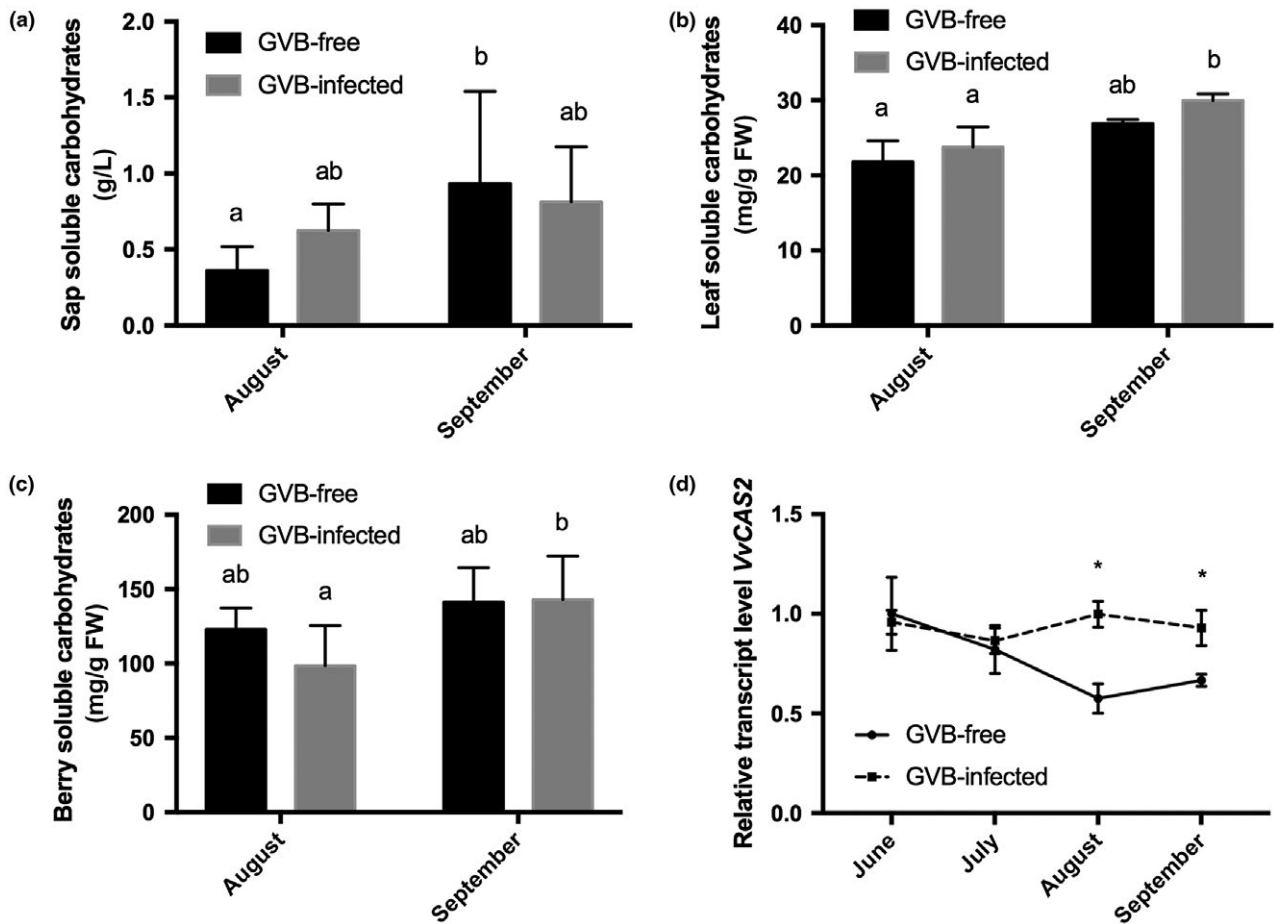


Fig. 3 Soluble carbohydrate content in sap (a), leaves (b) and berries (c) collected in 2016 at the end of August and at the end of September from grapevine virus B (GVB)-free (black columns) and GVB-infected (grey columns) plants. Data are mean values and bars are standard error (SE) ($n = 6$). (d) Seasonal changes in the relative expression levels of *VvCAS2* (VIT_06s0004g01270) obtained by quantitative reverse transcription-polymerase chain reaction (RT-PCR) on GVB-free (full line, filled circles) and GVB-infected (broken line, filled squares) leaves. Data are mean values and bars are SE ($n = 3$). Asterisks and lowercase letters denote significant differences attested by two-tailed Student's *t*-test and Tukey's honestly significant difference (HSD) test ($P < 0.05$), respectively.

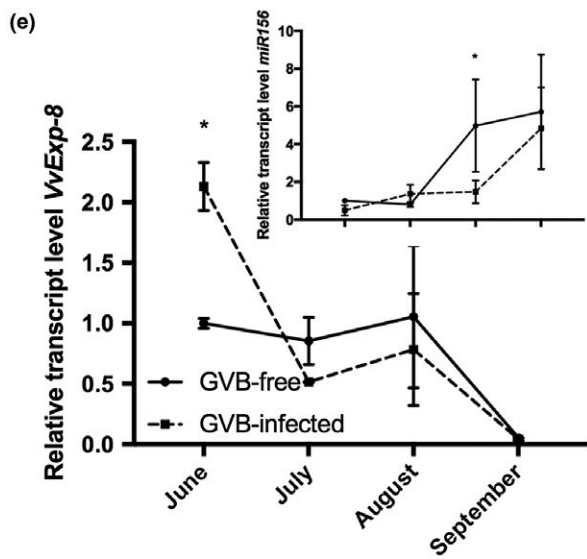
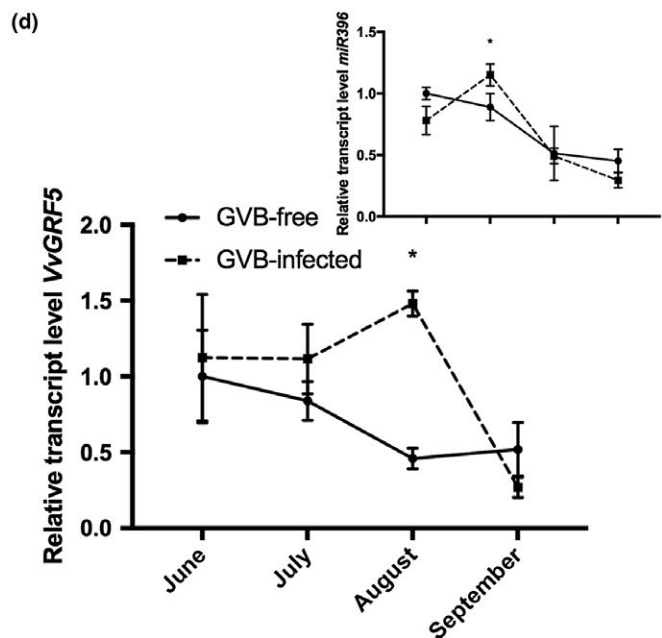
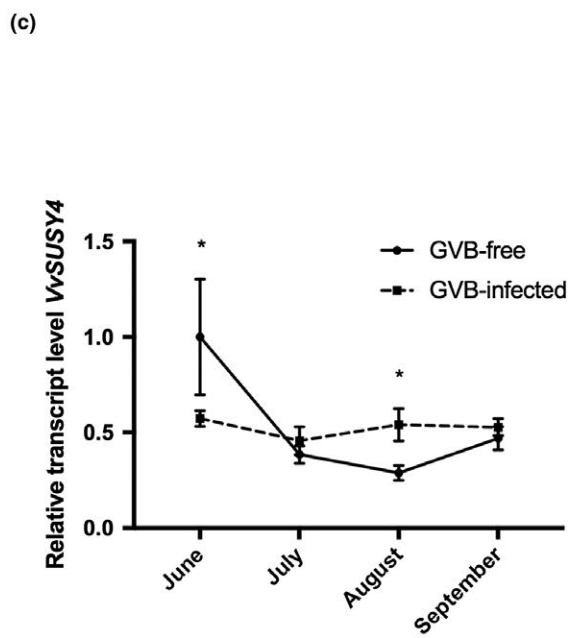
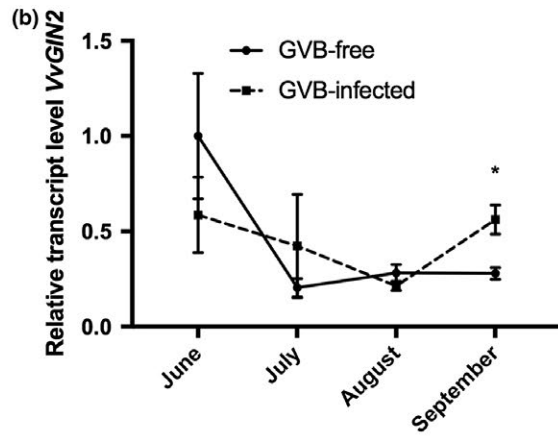
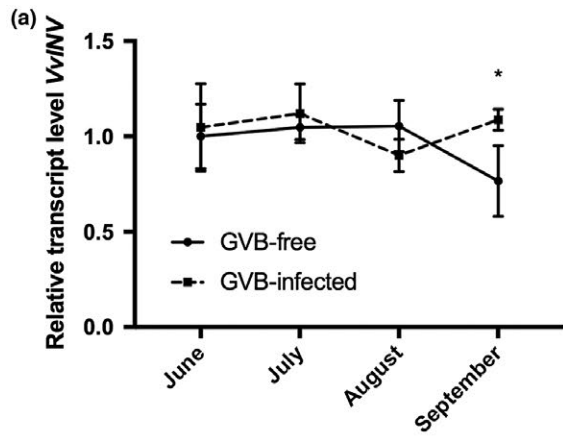


Fig. 4 Seasonal changes in the relative expression levels of (a) *VvINV* (VIT_09s0002g02320), (b) *VvGIN2* (VIT_02s0154g00090), (c) *VvSUSY4* (VIT_11s0016g00470), (d) miR396 (inset) and its target *VvGRF5* (VIT_16s0039g01450) and (e) miR156 (inset) and its target *VvExp-8* (VIT_13s0067g02930) measured by quantitative reverse transcription-polymerase chain reaction (RT-PCR) in grapevine virus B (GVB)-free (full line, filled circles) and GVB-infected (broken line, filled squares) leaves. Data are mean values and bars are standard error (SE) ($n = 3$). Asterisks denote significant differences attested by two-tailed Student's *t*-test ($P < 0.05$).

GVB-free plants at the end of the season, whereas no significant variations were observed in infected plants between August and September (Fig. 3a). Soluble carbohydrates determined in leaves and berries in August did not reveal significant differences in either GVB-free or GVB-infected samples. In contrast, a higher content of soluble carbohydrates was observed at the end of September in both GVB-infected leaves and berries (Fig. 3b,c).

To further investigate the potential role of sugars and, in particular, of sugar signalling in the tested conditions, a group of candidate genes related to sugar metabolism were analysed in leaves taken from GVB-infected and GVB-free plants. The expression level of the callose synthase gene *VvCAS2* (VIT_06s0004g01270) was significantly up-regulated at the end of August and September in GVB-infected vs. GVB-free samples (Fig. 3d). Conversely, over the season, both *VvINV* (VIT_09s0002g02320), encoding a cell wall invertase, and *VvGIN2* (VIT_02s0154g00090), encoding a vacuolar invertase, showed similar expression trends for infected and healthy vines, with the only exception of samples collected in September, where significant differences were observed between GVB-free and GVB-infected samples (Fig. 4a,b). The expression profile of the sucrose synthase gene *VvSUSY4* (VIT_11s0016g00470) was almost constant during the season in infected samples, whereas, in GVB-free leaves, its transcriptional profile followed a decreasing trend starting in July (Fig. 4c).

In addition to transcripts involved in sugar metabolism, two genes known to exert a role in leaf development were analysed. Transcripts of *VvGRF5* (VIT_16s0039g01450), encoding a growth regulating factor, were higher over time in GVB-infected plants, although significant differences were detected only at the end of August, followed by a strong decrease at the end of the season, reaching expression levels similar to those obtained for GVB-free vines (Fig. 4d). Furthermore, *VvGRF5* is a target of the conserved miRNA miR396, whose expression trend in infected samples was always opposite to its target gene, with the only exception being the last sampling point (Fig. 4d, inset). Conversely, in GVB-free samples, miR396 showed the same expression profile as its target (Fig. 4d, inset). The expression of *VvExp-8* (VIT_13s0067g02930), a gene involved in plant cell growth and development, was highly up-regulated in infected leaves at the beginning of the season (June) when compared with GVB-free samples; it then underwent a strong decrease, characterized by very low expression levels at the end of September when leaf senescence processes typically take place (Fig. 4e). *VvExp-8* is a target of the conserved miRNA miR156, whose accumulation

levels were always opposite to those of *VvExp-8* in both GVB-infected and GVB-free samples (Fig. 4e, inset).

Altogether, these data show that GVB activates sugar metabolism causing the accumulation of soluble carbohydrates in leaves and berries, as well as the expression of genes related to carbohydrate metabolism and cell wall development, particularly at the end of the season.

Anthocyanin profile and flavonoid-related genes in berries

'Albarossa' mature berries showed a very high ability to accumulate anthocyanins (up to 2.7 g/kg of grapes) with the prevalence of tri-hydroxylated forms. On a per weight basis (mg/kg of berries and mg/g of skins), GVB infection increased the anthocyanin concentration because of the significantly lower weight of berries and skins (Table 2). The concentrations of tri-hydroxylated free forms, of acetate and *p*-coumaroyl derivative forms and, consequently, of total acylated anthocyanins were significantly higher in GVB-infected berries (Table 2). In terms of concentration, the increase in acylated forms was ascribed to tri-hydroxylated and not di-hydroxylated anthocyanins. As expected, changes in the concentration of free tri-hydroxylated anthocyanins and of acylated forms were not sufficiently high to determine significant variations in the whole anthocyanin profile of GVB-infected berries. The only exception was represented by the percentage of di-hydroxylated acyl-anthocyanins, which decreased in infected berries because of the substantial stability of their concentration, regardless of the infection condition (Table 2). Overall, the profile (i.e. percentage incidence of individual anthocyanins over total anthocyanin concentration) was not influenced by the infection status, except for di-hydroxylated acyl-derivatives.

Patterns of anthocyanin accumulation were further analysed in berry tissues by monitoring the expression profiles of anthocyanin-related genes (Fig. 5). Transcripts encoding the MYB transcription factor *VvMybA1* (VIT_02s0033g00410) and the enzymes UDP-glucose flavonoid glucosyltransferase *VvUGT* (VIT_16s0039g02230) and anthocyanin acyltransferase *VvBAT* (VIT_03s0017g00870) displayed similar and overlapping expression patterns between healthy and infected samples, all characterized by a sharp peak of expression in August (Fig. 5a–c). More specifically, for these genes, the mRNA levels showed no significant difference between GVB-free and GVB-infected samples, although slightly higher expression levels were detected in infected berries, particularly at the last two sampling points (Fig. 5a–c). The same transcriptional profiles were observed

Table 2 Total anthocyanins (TA), berry and skin weights, and concentrations and profiles of anthocyanins grouped per class in grapevine virus B (GVB)-free and GVB-infected berries of 'Albarossa'.

	TA (mg/kg)	TA (mg/g skin)	Berry weight (g)	Skin weight (g)	Total free anthocyanin (mg/g skin)	Free tri-hydroxylated forms (mg/g skin)	Free di-hydroxylated forms (mg/g skin)	Total acyl-derivatives	Acetyl derivatives	p-Coumaroyl derivatives	Tri-hydroxylated acyl-derivatives	Di-hydroxylated acyl-derivatives
GVB-free	2.5 ± 0.04	32.0 ± 0.4	18.0 ± 0.3	0.14 ± 0.01	27.6 ± 1.7	21.9 ± 0.1	2.5 ± 0.1	7.6 ± 0.2	2.8 ± 0.1	4.8 ± 0.1	5.9 ± 0.1	1.7 ± 0.0
GVB-infected	2.7 ± 0.07	36.4 ± 1.8	16.4 ± 0.3	0.12 ± 0.01	24.4 ± 0.3	24.9 ± 1.4	2.8 ± 0.3	8.8 ± 0.3	3.3 ± 0.1	5.5 ± 0.2	7.0 ± 0.3	1.8 ± 0.1
Sig.	*	**	**	**	*	*	ns	**	*	**	**	ns

Values represent averages of three technical replicates per field replicate ($n = 3$). Significance amongst averages was evaluated by Tukey's honestly significant difference (HSD) test (* $P \leq 0.05$; ** $P \leq 0.01$; ns, non-significant).

in both conditions for two other selected genes encoding flavonoid 3'-hydroxylases: *VvF3'5'Hf* (VIT_06s0009g02860) and *VvF3'5'Hg* (VIT_06s0009g02810, VIT_06s0009g02840, VIT_06s0009g02880, VIT_06s0009g02920, VIT_06s0009g02970) (Fig. 5d,e). A strong increase in these transcripts was observed in August, followed by a decrease at harvest (Fig. 5d,e). Nevertheless, unlike the observations for the previously described genes, both *VvF3'5'Hf* and *VvF3'5'Hg* were significantly more expressed in August in the presence of the virus, according to the high accumulation of free tri-hydroxylated anthocyanins in infected samples (Table 2). Similarly, the expression of a gene encoding the 3'-hydroxylase *VvF3'Ha* (VIT_17s0000g07200) underwent a progressively increasing trend over the season in both groups of samples, with significantly higher transcript accumulation in GVB-infected berries at the end of August (Fig. 5f).

Therefore, GVB infection increased anthocyanin concentration in berries, and particularly the content of acylated forms, in agreement with the expression trends of *VvF3'5'Hf*, *VvF3'5'Hg* and *VvF3'Ha* genes.

DISCUSSION

During recent decades, particular attention has been paid to disease management, with plant pathogens being the main cause of losses in crop production. For these reasons, the need to dissect the complex network of factors at the base of the plant-pathogen-environment interaction has become an impelling issue for the scientific community. In this study, an integrated approach involving agronomic, physiological, biochemical and molecular analyses was adopted to investigate the performance of grapevine in response to GVB infection in a vineyard.

GVB infection triggers peculiar ecophysiological and molecular responses in leaves

Viruses are obligate intracellular agents that replicate exclusively in the symplast of their hosts and are able to move cell to cell to the vascular tissues. GVB is a phloem-limited virus and little information is available to date about its cell to cell movement, or for other members of the genus *Vitivirus* (Haviv *et al.*, 2012). Here, we have shown that the GVB concentration decreased over time in grapevine leaves and, in parallel, strongly increased in berry tissues, suggesting that its spread occurs particularly in sink organs (e.g. berries) and that the phloem is probably the main route of virus diffusion. Our results confirmed that GVB abundance can vary during the growing season, indicating that both climatic conditions and plant phenological stage play a key role in influencing virus movement within an infected vine and concentration, as indicated previously for other virus-grapevine genotype combinations (El Aou-ouad *et al.*, 2016; Gambino *et al.*, 2012; Montero *et al.*, 2017; Vega *et al.*, 2011; Velasco *et al.*, 2014). Of particular note, the GVB titre measured in 'Albarossa' berries was more than 1000 times higher than that in leaves collected

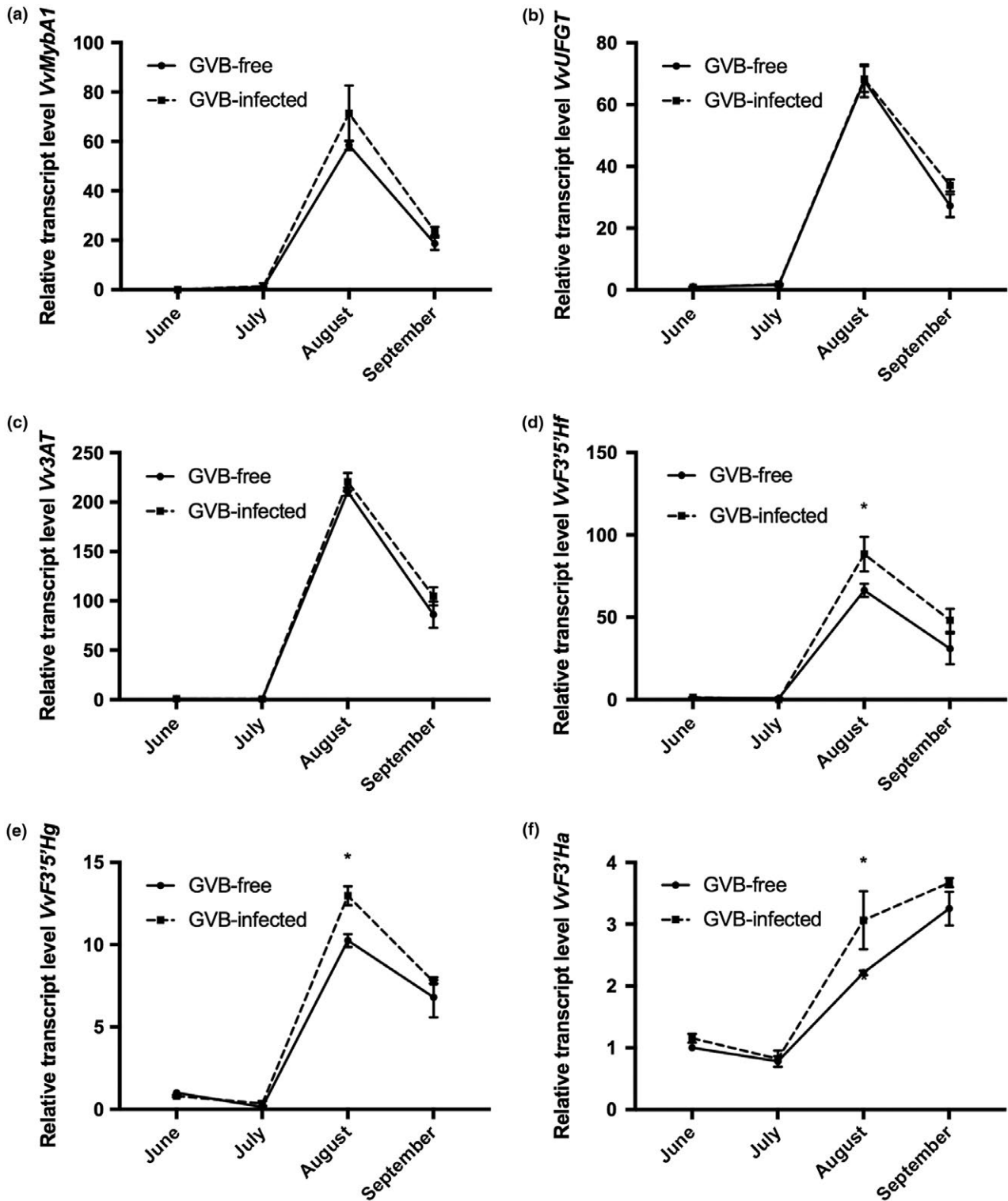


Fig. 5 Seasonal changes in the relative expression levels of (a) *VvMybA1* (VIT_02s0033g00410), (b) *VvUFGT* (VIT_16s0039g02230), (c) *Vv3AT* (VIT_03s0017g00870), (d) *VvF3'5'Hf* (VIT_06s0009g02860), (e) *VvF3'5'Hg* (VIT_06s0009g02810, VIT_06s0009g02840, VIT_06s0009g02880, VIT_06s0009g02920, VIT_06s0009g02970) and (f) *VvF3'Ha* (VIT_17s0000g07200), analysed by quantitative reverse transcription-polymerase chain reaction (RT-PCR) in grapevine virus B (GVB)-free (full line, filled circles) and GVB-infected (broken line, filled squares) berries. Data are mean values and bars are the standard error (SE) ($n = 3$). Asterisks denote significant differences attested by two-tailed Student's t -test ($P < 0.05$).

at the end of the season. These data are unique when compared with the quantification of other phloem-limited grapevine viruses. For instance, in GRSPaV-infected vines, the virus titre was only three to four times higher in berries than in leaves (Gambino *et al.*, 2012), whereas, in GLRaV-3-infected plants, the accumulation of viral RNAs increased in berries by the end of the season, but remained at least 10 times lower than that in the leaves (Vega *et al.*, 2011).

The environmental conditions during both experimental seasons were similar, as were the agronomic features. No significant differences were noted in terms of agronomic parameters when GVB-free and GVB-infected samples were compared, suggesting no or limited detrimental effects of GVB infection, at least in the tested vineyard conditions. Indeed, many factors, such as environmental conditions, virus strain and graft combination, can modulate the phenotypic alterations observed in GVB-infected grapes and the intensity of symptoms, as also reported for GVA-infected grapevines (Rosa *et al.*, 2011). In addition, in several infected rootstocks, including Kober 5BB, which was selected for this study, GVB exerts more adverse effects on plant growth in the presence of multiple infections, in particular in combination with GVA (Rosa *et al.*, 2011).

The analysis of leaf physiological performances attested that net photosynthesis, stomatal conductance and substomatal CO₂ concentration were the main parameters affected by GVB, particularly at the end of the season. Nevertheless, GVB-infected grapevines underwent a decrease in terms of physiological performance to a lesser extent than other grapevine–virus combinations (Guidoni *et al.*, 1997; Mannini *et al.*, 2012; Montero *et al.*, 2017; Sampol *et al.*, 2003). The overall picture of gas exchange measurements indicated a moderate metabolic, non-stomatal, photosynthetic limitation in GVB-infected plants in the absence of environmental and/or water limitation, in accordance with the results reported previously in GRSPaV-infected grapevines (Gambino *et al.*, 2012). Furthermore, the results revealed that infected plants experienced higher *c_i* rates at the end of the season, probably because of the slow down of the Calvin cycle, resulting in a metabolic hindrance to CO₂ diffusion in the mesophyll (Montero *et al.*, 2017; Sampol *et al.*, 2003). Looking at the biochemistry of photosynthesis, the Rubisco content was higher in GVB-infected plants, mainly at the end of August, consistent with the observations on the expression trends of the *VvRubisco activase* gene. The latter is a key regulator of the photosynthetic process, whose over-expression has been demonstrated previously to enhance the efficiency of the photosynthetic system by positively affecting the abundance of Rubisco (Parry *et al.*, 2003, 2012). In addition, the potential negative regulation driven by miR2950 on its target transcript, *VvChlorophyllase*, implied that the post-transcriptional inhibition of this gene could serve to limit damage to the photosynthetic apparatus in the presence of GVB infection. This supports the existence of a tight interaction

between miRNA-regulated pathways and physiological responses induced by the virus and, in general, by biotic and abiotic stress (Pantaleo *et al.*, 2016; Rodriguez *et al.*, 2010; Sunkar and Zhu, 2004; Xie *et al.*, 2012). The observed alterations in Rubisco content and the different modulation of photosynthesis-related genes induced by GVB could be interpreted as a mechanism to cope with the decrease in Pn rates, as well as a strategy to support viral replication and spread to sink organs, as suggested previously by Gambino *et al.* (2012).

The molecular interaction between GVB and 'Albarossa' goes beyond photosynthetic effects and could also involve the activity of conserved miRNAs related to plant development. Indeed, as observed in GVB-infected plants, the expression of two genes linked to cell growth and development, *VvGRF5* and *VvExp-8*, was affected during the season by the accumulation of miR396 and miR156, respectively. Lower expression levels of miR396 and miR156, respectively, coupled with opposite trends in the transcript profile of its target gene, *VvGRF5*, with an increase in the number of stomata and leaf abaxial surface cells, have been reported recently in GRSPaV-infected grapevines (Pantaleo *et al.*, 2016). miR156 was also down-regulated in GVB-free leaves, as observed in grapevines infected with GRSPaV (Pantaleo *et al.*, 2016), reinforcing the point that the occurrence of viral infection in grapevines can have detrimental effects on miR156 expression. It is worth noting that opposite quantitative RT-PCR profiles were not always observed between miRNAs and related transcripts in the collected samples. Nevertheless, it is conceivable that, in particular cases, such as in stress events often occurring in environmental conditions, expression changes in target mRNAs may not be directly associated with miRNA-mediated silencing effects, as other regulation mechanisms take over miRNA action, as already reported in grapevine (Pagliarani *et al.*, 2017). Further studies are undoubtedly needed to better understand the miRNA regulatory pathways triggered by the interaction between GVB, grapevine and the surrounding environment.

GVB infection alters biochemical processes linked to sugar metabolism and signalling

The plant carbohydrate partitioning is tightly regulated in terms of sink metabolic needs and its ability to retrieve assimilates (Naseem *et al.*, 2017). In addition, this system is strongly influenced by the plant sanitary status, as microbial pathogens (mainly fungi and bacteria), by using the nutrient-rich apoplast niche (sugars and metabolites), have evolved several strategies to proliferate and successfully infect the host (Toruno *et al.*, 2016). The host plant is able to perceive the phloem-inhabiting pathogens adopting a series of defence strategies to restrict them to the sieve elements, for example by depositing callose at plasmodesmata, as reported for phytoplasmas (Santi *et al.*, 2013) and viruses (Hong and Ju, 2017). Nevertheless, some viruses are

able to elude these defence mechanisms by inducing callose degradation to open the plasmodesmata and promote virus spread and symptom development (Bucher *et al.*, 2001). The inhibition of photosynthetic chain and Calvin cycle enzymes has been associated with the accumulation of soluble carbohydrates in leaves of *Phaseolus vulgaris* L. (Araya *et al.*, 2006) and in plants infected by phytoplasmas (André *et al.*, 2005; Maust *et al.*, 2003). Accordingly, in GVB-infected grapevines at the end of the season, together with lower Pn levels, slightly higher contents of soluble carbohydrates were observed, mainly in leaves, coupled with the up-regulation of a callose synthase gene (*VvCAS2*). Moreover, only healthy plants showed an increase in sap soluble carbohydrates at the end of the season. These findings support the hypothesis that GVB infection can induce effects of phloem loading inhibition, as well as effects reported in plants affected by phytoplasmas.

Some classes of oligosaccharide are well-known elicitors of plant defence mechanisms and are associated with the immune response in several plants (Prezelj *et al.*, 2016; Trouvelot *et al.*, 2014). Genes encoding sugar transporters and enzymes involved in sugar metabolism are commonly activated in response to phytoplasma infection, revealing the existence of some indirect effects of pathogens on sucrose metabolism in leaves (Hren *et al.*, 2009; Prezelj *et al.*, 2016; Santi *et al.*, 2013). Similarly, in GVB-infected plants, significantly higher expression levels of genes encoding an acidic vacuolar invertase, a cell wall invertase (*VvGIN2* and *VvINV*, respectively) and a sucrose synthase (*VvSUSY4*) were detected, particularly at the end of the season. This could represent a strategy for providing precursors for the rapid biosynthesis of callose plugs in the phloem vessel pores, as well as in the impairment of phloem loading, thus facilitating carbohydrate accumulation in the leaves, in accordance with previous findings in grapevines infected with *Flavescence dorée* (Prezelj *et al.*, 2016). In addition, a significant induction of a cell wall invertase gene has been observed previously in grapevine leaves exposed to fungus attack, in which the resulting reduction in phloem loading was responsible for the switching of leaves from source to sink organs (Hayes *et al.*, 2010). Interestingly, these biochemical responses overlap with those observed in grapevine under water stress conditions, in which the cell osmotic potential depends on the ratio between the activity of cytosolic enzymes (e.g. sucrose synthase) and cell wall invertases (e.g. *VvGIN2*). Indeed, the water stress-mediated activation of *VvGIN2*, reported by Medici *et al.* (2014), is related to a parallel increase in the cell osmotic potential addressed to maintain the vital metabolic functions of the plant by contributing to the sucrose balance between cytosol and vacuole compartments. It is thus highly probable that, in the analysed GVB-infected plants, a similar regulation of sugar metabolism-related genes occurs to successfully support the cell osmotic and metabolic functions.

All of these data corroborate the hypothesis that GVB infection, similar to the observations in GRSPaV-infected plants (Gambino *et al.*, 2012), impairs phloem loading and transport by callose deposition as a defence response strategy.

GVB infection positively affects anthocyanin accumulation and profiling in berries

As a consequence of a plant pathogen infection, a number of defence responses are activated in the host, including the synthesis of secondary metabolites in both sink and source organs (Prezelj *et al.*, 2016; Rojas *et al.*, 2014). During berry development, a progressive carbohydrate influx takes place in the berry to induce ripening metabolic processes, cell proliferation and expansion, as well as seed development (Coombe, 1992).

Our results suggest that GVB can affect grape development by influencing berry weight through a modification of soluble carbohydrate content, which increases in infected plant tissues. This could result from phloem flux limitation, a condition reported in GLRaV-3-infected grapevines (Montero *et al.*, 2016b). In red grape cultivars, such as 'Albarossa', anthocyanins are the main specific groups of flavonoids responsible for the red/purple colours of the skin (Schaefer *et al.*, 2004). In addition to other roles, anthocyanins are involved in protecting plants against both abiotic and biotic stresses (Ferrandino and Lovisolo, 2014; Margaria *et al.*, 2014; Prezelj *et al.*, 2016). Accordingly, all the analysed genes involved in anthocyanin biosynthesis were more strongly induced in GVB-infected berries over the ripening period, mirroring the anthocyanin accumulation obtained by high-performance liquid chromatography (HPLC) analysis on the same samples. In particular, higher concentrations of tri-hydroxylated free forms and of acylated anthocyanins were detected in infected mature berries. The accumulation of tri-hydroxylated anthocyanins, which represent the prevalent anthocyanin forms in 'Albarossa', is consistent with the over-expression of genes encoding flavonoid 3',5'-hydroxylases (*VvF3'5'H*). Moreover, 3',5'-hydroxylases (*VvF3'5'H*) and flavonoid 3'-hydroxylases (*VvF3'H*), which were both induced in infected berries, compete for the same substrate and are able to channel anthocyanin production into the branches, which leads to the synthesis of either tri-hydroxylated or di-hydroxylated free forms (Bogs *et al.*, 2006). Other GVB-mediated transcriptional changes include the activation of an anthocyanin acyltransferase gene (*Vv3AT*), already functionally characterized in grapevine and involved in the synthesis of the more stable acyl-derivative forms (Rinaldo *et al.*, 2015). An explanation for the higher induction of anthocyanin-related genes in GVB-infected than in GVB-free berries may also rely on the slight increase in soluble carbohydrates observed in both berry and leaf tissues. High contents of soluble carbohydrates are known to promote anthocyanin biosynthesis and probably also to modulate their profiles in specific tissues, as reported in *Arabidopsis*

and grapevine (Gollop *et al.*, 2002, 2001; Solfanelli *et al.*, 2006). It is of note that, although GVB infection does not damage carbohydrate and anthocyanin metabolism in 'Albarossa' berries, only negative effects on berry quality have been reported for other grapevine–virus associations. For example, GLRaV-3 induces a strong inhibition of carbohydrate and anthocyanin accumulation in berries (Alabi *et al.*, 2016; Guidoni *et al.*, 1997; Vega *et al.*, 2011). Similarly, mixed infections of GFLV + GFKV and of GLRaV-1 + GVA lead to a significant reduction in tri-hydroxylated malvidin-3-glucoside forms and in phenol extractability in 'Nebbiolo' grapes, with a negative impact on the overall wine quality (Santini *et al.*, 2011), whereas grapevine red blotch-associated virus (GRBaV) inhibits ripening, reducing the accumulation of pigments and flavours (Blanco-Ulate *et al.*, 2017).

CONCLUSIONS

GVB is associated with corky bark disorder. Here, we have shown that GVB infection affects grapevine photosynthesis via metabolic limitation (i.e. carbohydrate accumulation) because of the impairment in phloem flux of photoassimilates, without causing detrimental phenotypic alterations in terms of yield and plant vigour traits. These indirect GVB effects also trigger the modulation of key genes related to photosynthesis, sugar metabolism and development, as well as of some conserved miRNAs. We also documented that GVB infection causes changes in the metabolic profile of the berries by involving genes and metabolites of the anthocyanin branch which lead to enhanced accumulation of the more stable acyl-derivative forms, which are preferred for wine-making.

This is the first report of grapevine responses to GVB infection in the vineyard. Future studies are needed to further explore this interaction using different GVB isolates and *V. vinifera* cultivars, and by working either in different environments or under different stress conditions.

EXPERIMENTAL PROCEDURES

Vineyard, agronomic traits and sampling

The trials were carried out in a vineyard located in north-west Italy at the Cannona experimental station (Carpeneto, AL, Piedmont Region) during two consecutive years (2015 and 2016). Environmental conditions at the experimental vineyard are reported in Fig. S1. The vineyard was located in a viticultural area suitable for *V. vinifera* 'Albarossa' cultivation. The 'Albarossa' vines were grafted onto the rootstock Kober 5BB, trained to a vertical trellis system and *Guyot* pruned. Conventional agronomic and phytosanitary treatments were regularly performed during the two growing seasons.

All 'Albarossa' plants were derived by vegetative propagation from a single mother plant originally infected with GVB and

afterwards subjected to sanitation, with the exception of some plants which were maintained intentionally infected by the virus for experimental purposes. The sanitary status of all plants in the vineyard was checked in 2015 and 2016 employing a multiplex RT-PCR method (Gambino and Gribaudo, 2006) able to detect all the major viruses commonly infecting grapevine in Italy and other viticultural countries: ArMV, GFLV, GVB, GFKV, GVA, GLRaV-1, -2, -3. In order to characterize the isolate of GVB infecting 'Albarossa', the RT-PCR amplification products were purified and sequenced by Sanger sequencing, as reported previously (Gambino *et al.*, 2017). Forty-nine GVB sequences deposited in GenBank (National Center for Biotechnology Information, NCBI) were aligned with the 'Albarossa' isolate using Clustal Omega (<https://www.ebi.ac.uk/Tools/msa/clustalo/>), and phylogenetic analysis based on the neighbour-joining (NJ) method (with bootstrap values of 1000 replicates) was carried out using MEGA7 software (Kumar *et al.*, 2016).

Six GVB-infected and six GVB-free 'Albarossa' plants were randomly selected in the vineyard along two parallel rows. All vines were 6 years old and planted at a density of 3500 plants/ha. For each plant, berries and fully expanded leaves of a similar developmental stage, inserted in the central section of the shoot, were collected monthly, starting from the end of June to the end of September in 2016. For each condition (GVB-free and GVB-infected), three biological replicates, each made up of a pool of samples taken from two plants, were used for molecular analyses. In particular, for each of the two plants representing one biological replicate, three leaves and 30 berries were collected, immediately frozen in liquid nitrogen and stored at -80°C until molecular and biochemical analyses. Unlike molecular analyses, agronomic parameters, i.e. bunch weight and yield at harvest and pruning weight, were measured for each vine in 2015 and 2016.

Measurements of leaf gas exchange, stem water potential and leaf soluble carbohydrates

Leaf gas exchange rates were measured using an open gas exchange apparatus LCpro+ ADC (Analytical Development Company, Hoddesdon, Hertfordshire, UK) with a broad leaf chamber (leaf area, 6.25 cm^2). Measurements were taken in summer (June–September) once a month during a sunny day between 10:00 and 13:00 h under saturating light conditions [photosynthetic photon flux density (PPFD) was around $1400\text{--}1500\text{ }\mu\text{mol photons/m}^2/\text{s}$] and at ambient relative humidity (RH) and CO_2 values. Data were collected on three well-exposed fully formed leaves per plant (six plants for each condition) in the central section of the shoot.

Stem water potential (ψ_{stem}) was determined on leaves (one leaf/plant and condition) covered with aluminium foil and inserted in a humidified plastic bag for at least 1 h prior to excision. Afterwards, xylem pressure was measured using

a Scholander-type pressure chamber (Soil Moisture Equipment Corp., Santa Barbara, CA, USA).

The anthrone-sulfuric acid assay was used to quantify soluble carbohydrate content, as described by Leyva *et al.* (2008) and further modified by Secchi and Zwieniecki (2012). Measurements were performed on leaf, berry and xylem sap samples collected at the end of August and September in 2016. The xylem sap of vessels from the six GVB-infected and six GVB-free 'Albarossa' plants was collected using the procedure described previously by Secchi and Zwieniecki (2012).

Quantitative RT-PCR analysis in leaf and berry

Total RNA was extracted in triplicate from grapevine tissues collected in 2016 using the Spectrum™ Plant Total RNA Extraction Kit (Sigma-Aldrich, Inc., Saint Louis, MO, USA). RNA quantity and quality were checked using a NanoDrop 1000 spectrophotometer (Thermo Fisher Scientific, Waltham, MA, USA); then, samples were treated with DNase I (Invitrogen, Thermo Fisher Scientific) in accordance with the manufacturer's instructions. For each biological replicate, first-strand cDNA synthesis and real-time PCR were carried out as reported by Chitarra *et al.* (2017). The results were calculated as the expression ratios (relative quantity, RQ) relative to healthy plants.

Relative quantification of GVB was carried out on leaves and berries using primers designed on the viral RNA-dependent RNA polymerase and following the same procedure as reported above (Table S1, see Supporting Information).

Quantification of miRNA expression profiles (Table S1) was also performed by quantitative RT-PCR following the protocol of Pantaleo *et al.* (2016).

Anthocyanin profiling

Thirty berries per biological replicate were divided into subgroups of 10 berries each; berries were peeled and skins were extracted in a pH 3.2 ethanolic buffer, as described in Di Stefano and Cravero (1991). Anthocyanins were separated from sugar residues and other polyphenols by solid phase extraction onto C18 cartridges (Sep-Pak®, Waters Corporation, Milford, MA, USA) and eluted with methanol. The methanolic extract was evaporated to dryness (Laborota 4000, Heidolph Instruments GmbH and Co., Schwabach, Germany) under reduced pressure at 35 °C and resuspended in solvent B. Extracts were filtered through a 0.20-µm hydrophilic polypropylene filter (Acrodisc® Syringe Filter, PALL Corporation, Hempstead, NY, USA). Analytical separation of anthocyanins was performed using a 1260 Infinity HPLC-DAD system (Agilent Technologies, Santa Clara, CA, USA) equipped with a Lichrocart® 250-4 HPLC-Cartridge Purospher® STAR RP-18 (5 mm) with a guard column, operating at 30 °C. The mobile phase consisted of water–formic acid (90 : 10, v/v; eluent A) and methanol–formic acid–water (50 : 10 : 40, v/v/v; eluent B)

with the following gradient: from 72% to 55%, 15 min; to 30%, 20 min; to 10%, 10 min; to 1%, 5 min; to 72%, 3 min. The flow was set at 1 mL/min. Individual anthocyanins were identified by comparing retention times and DAD spectra with those of pure molecules, when available, and/or by comparison with published spectra.

Rubisco analysis

To analyse Rubisco content, 1 g of leaf sample collected at two time points during the vegetative season (August and September 2016), and maintained at –80 °C, was ground to a fine powder using liquid nitrogen. The powder was added to 10 mL of cold lysis buffer [50 mM TRIS-HCl, pH 7.5, 2 M thiourea, 7 M urea, 2% (v/v) Triton X-100, 1% dithiothreitol (DTT), 2% (w/v) soluble polyvinylpyrrolidone (PVPP), 1 mM phenylmethylsulfonyl fluoride (PMSF)], purified and precipitated using a trichloroacetic acid–acetone method, as described previously (Margarita and Palmano, 2011). The total protein content was determined spectrophotometrically according to Bradford (1976), using bovine serum albumin as standard.

To determine Rubisco amount by densitometry, 5 µg of total proteins were separated by sodium dodecylsulfate-polyacrylamide gel electrophoresis (SDS-PAGE) with a Mini-ProteanII System (Bio-Rad, Hercules, CA, USA) in Laemmli buffer. Gels were treated in fixing buffer (40% v/v ethanol, 20% v/v acetic acid), stained overnight with colloidal Coomassie blue (0.75 M ammonium sulfate, 10% v/v orthophosphoric acid, 0.12% w/v Brilliant Blue G, 25% v/v methanol) and finally rinsed in water to remove excess stain. Gels were captured with a VersaDoc imaging system (Bio-Rad) and images were analysed by Quantity One software (Bio-Rad).

Statistical analysis

Data on the agronomic traits monitored in the 2 years were analysed separately and one-way analysis of variance (ANOVA), with sanitary status and/or sampling time as the main factor, was performed using the SPSS statistical software package v. 23.0 (SPSS Inc., Cary, NC, USA). Tukey's honestly significant difference (HSD) test was used when ANOVA showed significant differences ($P < 0.05$). Significant differences in pairwise comparisons were assessed by Student's *t*-test. The standard deviation (SD) and standard error (SE) of all means were calculated.

ACKNOWLEDGEMENTS

I.P. acknowledges funding by the Italian Ministry of Education, University and Research (MIUR), FIR project RBF13GHC5: 'The epigenomic plasticity of grapevine in genotype per environment interactions'. We are grateful to Centro Sperimentale 'Tenuta Cannona' – AGRION, Carpeneto (AL), for management of the experimental vineyard.

COMPETING INTERESTS

The authors declare no conflicts of interest.

AUTHOR CONTRIBUTIONS

W.C. planned and designed the research, performed most of the experiments, analysed the data and wrote the article. A.F. carried out the HPLC assays, analysed the corresponding data and complemented the writing. D.C. collaborated in the physiological experiments, analysed the data and revised the article. F.S. contributed to the physiological analyses and sampling, and analysed the related data. S.P. carried out Rubisco analysis and complemented the writing. I.P., P.B. and C.P. contributed to the molecular analysis, revised the manuscript and complemented the writing. I.G. and F.M. critically revised the manuscript and complemented the writing. G.G. conceived the project, supervised all the experiments, wrote the article and critically revised the manuscript. All authors read and approved the final manuscript.

REFERENCES

- Alabi, O.J., Casassa, L.F., Gutha, L.R., Larsen, R.C., Henick-Kling, T., Harbertson, J.F. and Naidu, R.A.** (2016) Impacts of grapevine leafroll disease on fruit yield and grape and wine chemistry in a wine grape (*Vitis vinifera* L.) cultivar. *PLoS One*, **11**, e0149666.
- André, A., Maucourt, M., Moing, A., Rolin, D. and Renaudin, J.J.** (2005) Sugar import and phytopathogenicity of *Spiroplasma citri*: glucose and fructose play distinct roles. *Mol. Plant–Microbe Interact.* **18**, 33–42.
- Araya, T., Noguchi, K. and Terashima, I.** (2006) Effects of carbohydrate accumulation on photosynthesis differ between sink and source leaves of *Phaseolus vulgaris* L. *Plant Cell Physiol.* **47**, 644–652.
- Armijo, G., Schlechter, R., Agurto, M., Muñoz, D., Nuñez, C. and Arce-Johnson, P.** (2016) Grapevine pathogenic microorganisms: understanding infection strategies and host response scenarios. *Front. Plant Sci.* **7**, 382.
- Blanco-Ulate, B., Hopfer, H., Figueroa-Balderas, R., Ye, Z., Rivero, R.M., Albacete, A., Perez-Alfocea, F., Koyama, R., Anderson, M.M., Smith, R.J., Ebeler, S.E. and Cantu, D.** (2017) Red blotch disease alters grape berry development and metabolism by interfering with the transcriptional and hormonal regulation of ripening. *J. Exp. Bot.* **68**, 1225–1238.
- Bogs, J., Ebadi, A., McDavid, D. and Robinson, P.** (2006) Identification of the flavonoid hydroxylases from grapevine and their regulation during fruit development. *Plant Physiol.* **140**, 279–291.
- Bradford, M.M.** (1976) A rapid and sensitive method for the quantitation of microgram quantities of protein utilizing the principle of protein–dye binding. *Anal. Biochem.* **72**, 248–254.
- Bucher, G.L., Tarina, C., Heinlein, M., Di Serio, F., Meins, F. and Iglesias, V.A.** (2001) Local expression of enzymatically active class I beta-1,3-glucanase enhances symptoms of TMV infection in tobacco. *Plant J.* **28**, 361–369.
- Chitarra, W., Perrone, I., Avanzato, C.G., Minio, A., Boccacci, P., Santini, D., Gilardi, G., Siciliano, I., Gullino, M.L., Delledonne, M., Mannini, F. and Gambino, G.** (2017) Grapevine grafting: scion transcript profiling and defense-related metabolites induced by rootstocks. *Front. Plant Sci.* **8**, 654.
- Coombe, B.** (1992) Research on the development and ripening of the grape berry. *Am. J. Enol. Viticult.* **43**, 101–110.
- Csorba, T., Pantaleo, V. and Burgyan, J.** (2009) RNA silencing: an antiviral mechanism. *Adv. Virus Res.* **75**, 35–71.
- Dessaux, Y., Granclément, C. and Faure, D.** (2016) Engineering the rhizosphere. *Trends Plant Sci.* **21**, 266–278.
- Di Stefano, R. and Cravero, M.C.** (1991) Metodo per lo studio dei polifenoli dell'uva. *Riv. Vit. Enol.* **44**, 37–45.
- Dicke, M.** (2016) Plant phenotypic plasticity in the phytobiome: a volatile issue. *Curr. Opin. Plant Biol.* **32**, 17–23.
- El Aou-ouad, H., Montero, R., Medrano, H. and Bota, J.** (2016) Interactive effects of grapevine leafroll-associated virus 3 (GLRaV-3) and water stress on the physiology of *Vitis vinifera* L. cv. Malvasia de Banyalbufar and Giro-Ros. *J. Plant Physiol.* **196**, 106–115.
- Endeshaw, S.T., Sabbatini, P., Romanazzi, G., Schilder, A.C. and Neri, D.** (2014) Effects of grapevine leafroll associated virus 3 infection on growth, leaf gas exchange, yield and basic chemistry of *Vitis vinifera* L. cv. Cabernet Franc. *Sci. Hortic.-Amsterdam*, **170**, 228–236.
- Ferrandino, A. and Lovisolo, C.** (2014) Abiotic stress effects on grapevine (*Vitis vinifera* L.): focus on abscisic acid-mediated consequences on secondary metabolism and berry quality. *Environ. Exp. Bot.* **103**, 138–147.
- Fonseca, F., Duarte, V., Teixeira Santos, M., Brazão, J. and Eiras-Dias, E.** (2016) First molecular characterization of grapevine virus B (GVB) in Portuguese grapevine cultivars and improvement of the RT-PCR detection assay. *Arch. Virol.* **161**, 3535–3540.
- Gambino, G., Cuozzo, D., Fasoli, M., Pagliarani, C., Vitali, M., Boccacci, P., Pezzotti, M. and Mannini, F.** (2012) Co-evolution between *Grapevine rupestris stem pitting-associated virus* and *Vitis vinifera* L. leads to decreased defence responses and increased transcription of genes related to photosynthesis. *J. Exp. Bot.* **63**, 5919–5933.
- Gambino, G., Dal Molin, A., Boccacci, P., Minio, A., Chitarra, W., Avanzato, C.G., Tononi, P., Perrone, I., Raimondi, S., Schneider, A., Pezzotti, M., Mannini, M., Gribaudo, I. and Delledonne, M.** (2017) Whole-genome sequencing and SNV genotyping of 'Nebbiolo' (*Vitis vinifera* L.) clones. *Sci. Rep.* **7**(1), 17294.
- Gambino, G. and Gribaudo, I.** (2006) Simultaneous detection of nine grapevine viruses by multiplex RT-PCR with coamplification of a plant RNA internal control. *Phytopathology*, **96**, 1223–1229.
- Gollop, R., Even, S., Colova-Tsolova, V. and Perl, A.** (2002) Expression of the grape dihydroflavonoid reductase gene and analysis of its promoter region. *J. Exp. Bot.* **53**, 1397–1409.
- Gollop, R., Farhi, S. and Perl, A.** (2001) Regulation of the leucoanthocyanidin dioxygenase gene expression in *Vitis vinifera*. *Plant Sci.* **161**, 579–588.
- Goszczynski, D.E.** (2010) Divergent molecular variants of Grapevine virus B (GVB) from corky bark (CB)-affected and CB-negative LN33 hybrid grapevines. *Virus Genes*, **41**, 273–281.
- Guidoni, S., Mannini, F., Ferrandino, A., Argamante, N. and Di Stefano, R.** (1997) The effect of grapevine leafroll and rugose wood sanitation on agronomic performance and berry and leaf phenolic content of a Nebbiolo clone (*Vitis vinifera* L.). *Am. J. Enol. Viticult.* **48**, 438–442.
- Gutha, L.R., Casassa, L.F., Harbertson, J.F. and Rayapati, A.N.** (2010) Modulation of flavonoid biosynthetic pathway genes and anthocyanins due to virus infection in grapevine (*Vitis vinifera* L.) leaves. *BMC Plant Biol.* **10**, 187.

- Haviv, S., Moskovitz, Y. and Mawassi, M.** (2012) The ORF3-encoded proteins of vitiviruses GVA and GVB induce tubule-like and punctate structures during virus infection and localize to the plasmodesmata. *Virus Res.* **163**, 291–301.
- Hayes, A., Feechan, A. and Dry, I.B.** (2010) Involvement of abscisic acid in the coordinated regulation of a stress-inducible hexose transporter (*VvHT5*) and a cell wall invertase in grapevine in response to biotrophic fungal infection. *Plant Physiol.* **153**, 211–221.
- Hipper, C., Brault, V., Ziegler-Graff, V. and Revers, F.** (2013) Viral and cellular factors involved in phloem transport of plant viruses. *Front. Plant Sci.* **4**, 154.
- Hong, J. and Ju, H.** (2017) The plant cellular systems for plant virus movement. *Plant Pathol. J.* **33**, 213–228.
- Hren, M., Nikolic, P., Rotter, A., Blejec, A., Terrier, N., Ravnkar, M., Dermastia, M. and Gruden, K.** (2009) Bois noir phytoplasma induces significant reprogramming of the leaf transcriptome in the field grown grapevine. *BMC Genomics*, **10**, 460.
- Huang, J., Yang, M., Lu, L. and Zhang, X.** (2016) Diverse functions of small RNAs in different plant–pathogen communications. *Front. Microb.* **7**, 1552.
- Kumar, S., Stecher, G. and Tamura, K.** (2016) MEGA7: Molecular Evolutionary Genetics Analysis version 7.0 for bigger datasets. *Mol. Biol. Evol.* **33**, 1870–1874.
- Leyva, A., Quintana, A., Sanchez, M., Rodriguez, E.N., Cremata, J. and Sanchez, J.C.** (2008) Rapid and sensitive anthrone-sulfuric acid assay in microplate format to quantify carbohydrate in biopharmaceutical products: method development and validation. *Biologicals*, **36**, 134–141.
- Mannini, F. and Digiario, M.** (2017) The effects of viruses and viral diseases on grapes and wine. In: *Grapevine Viruses: Molecular Biology, Diagnostics and Management* (Meng, B., ed.), pp. 453–482. Cham (ZG): Springer International Publishing AG.
- Mannini, F., Mollo, A. and Credi, R.** (2012) Field performance and wine quality modification in clone of *Vitis vinifera* cv. Dolcetto after GLRaV-3 elimination. *Am. J. Enol. Viticult.* **63**, 144–147.
- Margarita, P., Ferrandino, A., Caciagli, P., Kedrina, O., Schubert, A. and Palmano, S.** (2014) Metabolic and transcript analysis of the flavonoid pathway in diseased and recovered Nebbiolo and Barbera grapevines (*Vitis vinifera* L.) following infection by *Flavescence dorée* phytoplasma. *Plant Cell Environ.* **37**, 2183–2200.
- Margarita, P. and Palmano, S.** (2011) Response of the *Vitis vinifera* L. cv. 'Nebbiolo' proteome to *Flavescence dorée* phytoplasma infection. *Proteomics*, **11**, 212–224.
- Márquez, L.M., Redman, R.S., Rodriguez, R.J. and Roossinck, M.J.** (2007) A virus in a fungus in a plant: three-way symbiosis required for thermal tolerance. *Science*, **315**, 513–515.
- Martelli, G.P.** (2017) An overview on grapevine viruses, viroids, and the diseases they cause. In: *Grapevine Viruses: Molecular Biology, Diagnostics and Management* (Meng, B., ed.), pp. 31–46. Cham: Springer International Publishing AG.
- Martelli, G.P.** (2018) Where grapevine virology is heading to. Proceedings of the 19th Congress of International Council for the Study of Viruses and Virus-like Diseases of the Grapevine, Santiago, Chile, 10–15.
- Maust, B.E., Espadas, F., Talavera, C., Aguilar, M., Santamaria, J.M. and Oropeza, C.** (2003) Changes in carbohydrate metabolism in coconut palms infected with the lethal yellowing phytoplasma. *Phytopathology*, **93**, 976–981.
- Medici, A., Laloi, M. and Atanassova, R.** (2014) Profiling of sugar transporter genes in grapevine coping with water deficit. *FEBS Lett.* **588**, 3989–3997.
- Miozzi, L., Gambino, G., Burgyan, J. and Pantaleo, V.** (2013) Genome-wide identification of viral and host transcripts targeted by viral siRNAs in *Vitis vinifera*. *Mol. Plant Pathol.* **14**, 30–43.
- Montero, R., El aou ouad, H., Pacifico, D., Marzachi, C., Castillo, N., Garcia, E., Del Saz, N.L., Florez-Sarasa, I., Flexas, J. and Bota, J.** (2017) Effects of grapevine leafroll-associated virus 3 on the physiology in asymptomatic plants of *Vitis vinifera*. *Ann. Appl. Biol.* **171**, 155–171.
- Montero, R., Mundy, D., Albright, A., Grose, C., Trought, M.C.T., Cohen, D., Chooi, K.M., MacDiarmid, R., Flexas, J. and Bota, J.** (2016b) Effects of *Grapevine Leafroll associated Virus 3* (GLRaV-3) and duration of infection on fruit composition and wine chemical profile of *Vitis vinifera* L. cv. *Sauvignon blanc*. *Food Chem.* **197**, 1177–1183.
- Montero, R., Pérez-Bueno, M.L., Barón, M., Florez-Sarasa, I., Tohge, T., Fernie, A.R., El Ouad, A., Flexas, J. and Bota, J.** (2016a) Alterations in primary and secondary metabolism in *Vitis vinifera* 'Malvasia de Banyalbufar' upon infection with *Grapevine Leafroll associated Virus 3* (GLRaV-3). *Physiol. Plant.* **157**, 442–452.
- Moon, J.Y. and Park, J.M.** (2016) Cross-talk in viral defense signaling in plants. *Front. Microbiol.* **7**, 2068.
- Moskovitz, Y., Goszczynski, D.E., Bir, L., Fingstein, A., Czosnek, H. and Mawassi, M.** (2008) Sequencing and assembly of a full-length infectious clone of grapevine virus B and its infectivity on herbaceous plants. *Arch. Virol.* **153**, 323–328.
- Naseem, M., Kunz, M. and Dandekar, T.** (2017) Plant-pathogen maneuvering over apoplastic sugars. *Trends Plant Sci.* **22**, 740–743.
- Nerva, L., Varese, G.C., Falk, B.W. and Turina, M.** (2017) Mycoviruses of an endophytic fungus can replicate in plant cells: evolutionary implications. *Sci. Rep.* **7**, 1908.
- Pagliarani, C., Vitali, M., Ferrero, M., Vitulo, N., Incarbone, M., Lovisolo, C., Valle, G. and Schubert, A.** (2017) The accumulation of miRNAs differentially modulated by drought stress is affected by grafting in grapevine. *Plant Physiol.* **173**, 2180–2195.
- Pantaleo, V., Vitali, M., Boccacci, P., Miozzi, L., Cuozzo, D., Chitarra, W., Mannini, F., Lovisolo, C. and Gambino, G.** (2016) Novel functional microRNAs from virus-free and infected *Vitis vinifera* plants under water stress. *Sci. Rep.* **6**, 20167.
- Parry, M.A.J., Andralojc, P.J., Mitchell, R.A., Madgwick, P.J. and Keys, A.J.** (2003) Manipulation of Rubisco: the amount, activity, function and regulation. *J. Exp. Bot.* **54**, 1321–1333.
- Parry, M.A.J., Andralojc, P.J., Scales, J.C., Salvucci, M.E., Carmo-Silva, A.E., Alonso, H. and Whitney, S.M.** (2012) Rubisco activity and regulation as target for crop improvement. *J. Exp. Bot.* **64**, 717–730.
- Perrone, I., Chitarra, W., Boccacci, P. and Gambino, G.** (2017) Grapevine–virus–environment interactions: an intriguing puzzle to solve. *New Phytol.* **213**, 983–987.
- Pradeu, T.** (2016) Mutualistic viruses and the heteronomy of life. *Stud. Hist. Philos. Sci.* **59**, 80–88.
- Prezelj, N., Covington, E., Roitsch, T., Gruden, K., Fragner, L., Weckwerth, W., Chersicola, M., Vodopivec, M. and Dermastia, M.** (2016) Metabolic consequences of infection of grapevine (*Vitis vinifera* L.) cv. "Modra frankinja" with *Flavescence Dorée* phytoplasma. *Front. Plant Sci.* **7**, 711.
- Pumplin, N. and Voinnet, O.** (2013) RNA silencing suppression by plant pathogens: defence, counter-defence and counter-counter-defence. *Nat. Rev. Microbiol.* **11**, 745–760.
- Repetto, O., Bertazzon, N., De Rosso, M., Miotti, L., Flamini, R., Angelini, E. and Borgo, M.** (2012) Low susceptibility of grapevine

- infected by GLRaV-3 to late *Plasmopara viticola* infections: towards understanding the phenomenon. *Physiol. Mol. Plant*, **79**, 55–63.
- Rinaldo, A., Cavallini, E., Jia, Y., Moss, S.M.A., McDavid, D.A.J., Hooper, L.C., Robinson, S.P., Tornielli, G.B., Zenoni, S., Ford, C.M., Boss, P.K. and Walker, A.R.** (2015) A grapevine anthocyanin acyltransferase, transcriptionally regulated by VvMYBA, can produce most acylated anthocyanins present in grape skins. *Plant Physiol.* **169**, 1897–1916.
- Rodriguez, R.E., Mecchia, M.E., Debernardi, J.M., Schommer, C., Weigel, D. and Palatnik, J.F.** (2010) Control cell proliferation in *Arabidopsis thaliana* by microRNA miR396. *Development*, **137**, 103–112.
- Rojas, C.M., Senthil-Kumar, M., Tzin, V. and Mysore, K.S.** (2014) Regulation of primary metabolism during plant–pathogen interactions and its contribution to plants. *Front. Plant Sci.* **5**, 17.
- Roossinck, M.J.** (2011) The good viruses: viral mutualistic symbioses. *Nat. Rev. Microbiol.* **9**, 99–108.
- Roossinck, M.J.** (2012) Persistent plant viruses: molecular hitchhikers or epigenetic elements? In: *Viruses: Essential Agents of Life* (Witzany, G., ed.), pp. 177–186. Dordrecht: Springer.
- Roossinck, M.J.** (2015) Move over, bacteria! Viruses make their mark as mutualistic microbial symbionts. *J. Virol.* **89**, 6532–6535.
- Rosa, C., Jimenez, J.F., Margaria, P. and Rowhani, A.** (2011) Symptomatology and effects of viruses associated with rugose wood complex on the growth of four different rootstocks. *Am. J. Enol. Viticult.* **62**, 207–213.
- Ruiz-Ferrer, V. and Voinnet, O.** (2009) Roles of plant small RNAs in biotic stress responses. *Annu. Rev. Plant Biol.* **60**, 485–510.
- Sampol, B., Bota, J., Riera, D., Medrano, H. and Flexas, J.** (2003) Analysis of the virus-induced inhibition of photosynthesis in malmsey grapevines. *New Phytol.* **160**, 403–412.
- Santi, S., Grisan, S., Pierasco, A., De Marco, F. and Musetti, R.** (2013) Laser microdissection of grapevine leaf phloem infected by stolbur reveals site-specific gene responses associated to sucrose transport and metabolism. *Plant Cell Environ.* **36**, 343–355.
- Santini, D., Rolle, L., Cascio, P. and Mannini, F.** (2011) Modifications in chemical, physical and mechanical properties of Nebbiolo (*Vitis vinifera* L.) grape berries induced by mixed virus infection. *S. Afr. J. Enol. Viticult.* **32**, 183.
- Schaefer, H.M., Schaefer, V. and Levey, D.J.** (2004) How plant–animal interactions signal new insights in communication. *Trends Ecol. Evol.* **19**, 577–584.
- Secchi, F. and Zwieniecki, M.A.** (2012) Analysis of xylem sap from functional (nonembolized) and nonfunctional (embolized) vessels of *Populus nigra*: chemistry of refilling. *Plant Physiol.* **160**, 955–964.
- Shapiro, L.R., Salvaudon, L., Mauck, K.E., Pulido, H., DeMoraes, C.M., Stephenson, A.G. and Mescher, M.C.** (2013) Disease interactions in a shared host plant: effects of pre-existing viral infection on cucurbit plant defense responses and resistance to bacterial wilt disease. *PLoS One*, **8**, e77393.
- Solfanelli, C., Poggi, A., Loreti, E., Alpi, A. and Perata, P.** (2006) Sucrose-specific induction of the anthocyanin biosynthetic pathway in *Arabidopsis*. *Plant Physiol.* **140**, 637–646.
- Sunkar, R. and Zhu, J.K.** (2004) Novel and stress-regulated microRNAs and other small RNAs from *Arabidopsis*. *Plant Cell*, **16**, 2001–2019.
- Toruno, T.Y., Stergiopoulos, I. and Coaker, G.** (2016) Plant-pathogen effectors: cellular probes interfering with plant defenses in spatial and temporal manner. *Annu. Rev. Phytopathol.* **54**, 419–441.
- Trouvelot, S., Héloir, M.C., Poinsot, B., Gauthier, A., Paris, F., Guiller, C., Combiér, M., Trdá, L., Daire, X. and Adrian, M.** (2014) Carbohydrates in plant immunity and plant protection: roles and potential application as foliar sprays. *Front. Plant Sci.* **5**, 592.
- Vega, A., Gutiérrez, R.A., Peña-Neira, A., Cramer, G.R. and Arce-Johnson, P.** (2011) Compatible GLRaV-3 viral infections affect berry ripening decreasing sugar accumulation and anthocyanin biosynthesis in *Vitis vinifera*. *Plant Mol. Biol.* **77**, 261–274.
- Velasco, L., Bota, J., Montero, R. and Cretazzo, E.** (2014) Differences of three ampeloviruses multiplication in plants contribute to explain their incidences in vineyards. *Plant Dis.* **98**, 395–400.
- Wang, A.** (2015) Dissecting the molecular network of virus–plant interactions: the complex roles of host factors. *Annu. Rev. Phytopathol.* **53**, 45–66.
- Xie, C., Zhang, R., Qu, Y., Miao, Z., Zhang, Y., Shen, X., Wang, T. and Dong, J.** (2012) Overexpression of MtCAS31 enhances drought tolerance in transgenic *Arabidopsis* by reducing stomatal density. *New Phytol.* **195**, 124–135.
- Xu, P., Chen, F., Mannas, J.P., Feldman, T., Summer, L.W. and Roossinck, M.J.** (2008) Virus infection improves drought tolerance. *New Phytol.* **180**, 911–921.
- Zhao, J., Zhang, X., Hong, Y. and Liu, Y.** (2016) Chloroplast in plant–virus interaction. *Front. Microbiol.* **7**, 1565.

SUPPORTING INFORMATION

Additional supporting information may be found in the online version of this article at the publisher's web site:

Fig. S1 Seasonal time courses (2015 and 2016) of maximum temperature, midday vapour pressure deficit and rainfall at the Cannona experimental station (Piedmont, North-Western Italy).

Fig. S2 Phenotype of the GVB-free and GVB-infected 'Albarossa' vines selected for this study.

Fig. S3 The Neighbour-Joining tree of several GVB isolates.

Fig. S4 Seasonal time course of stem water potential in 2016 (Ψ_{stem}).

Fig. S5 SDS-PAGE on the total protein extracts from GVB-infected and GVB-free grapevine leaf samples.

Table S1 List of the oligonucleotides used in this study.